Imaging Techniques for Corneal Disorders

4

Alla Kelly, Stephen C. Kaufman, Jonathan Lass, Denice Barsness, Beth Ann Benetz, and Pankaj Gupta

4.1 Introduction

Corneal imaging has developed dramatically since the seventeenth century where Christopher Scheiner reflected images of marbles off the cornea (Naroo and Cervino 2004). Now, technologies such as confocal microscopy, anterior segment optical coherence tomography (OCT), and specular microscopy allow imaging and analysis of both healthy and now diseased eyes which would be previously unable to be evaluated with just the marble. These imaging modalities allow us to evaluate microscopic diseases such as atypical infectious keratitis, Fuchs endothelial corneal dystrophy, and even attachment of endothelial keratoplasty.

A. Kelly, MD • S.C. Kaufman, MD, PhD
Department of Ophthalmology, University of Minnesota, Minneapolis, MN, USA

J. Lass, MD • B.A. Benetz, CRA, FOPS
P. Gupta, MD, MS (✉)
Department of Ophthalmology and Visual Sciences, Case Western Reserve University, Cleveland, OH, USA
e-mail: pankaj.gupta2@uhhospitals.org

D. Barsness, CRA, COMT, ROUB, CDOS, FOPS
Department of Ophthalmology Ophthalmic Diagnostic Center, California Pacific Medical Center, San Francisco, CA, USA

4.2 Confocal Microscopy

The confocal microscope allows in vivo coronal optical sectioning of the cornea. The first confocal scanning laser microscope was described by Petran et al. (1968). This microscope was capable of high-resolution images of cells within tissues. The confocal microscope can capture 2–20 μm optical sections oriented parallel to the tissue surface, without stains or dyes.

4.2.1 Function

The conventional light microscope collects the sum of all light transmitted through a specimen or reflected back from an object, along with light from above and below the focal plane of the microscope's objective lens. This creates optical noise, which results in blurred images with significantly limited resolution. Consequently, to improve the resolution, the specimen needs to be thinly sliced. This need to physically section the specimen, and apply tissue stains, clearly does not allow in vivo imaging and may result in preparation artifacts.

In confocal microscopy, as first described by Minsky in his patent in 1957 (Minsky 1988), the pinhole source of light and its conjugate pinhole detector limit the passage of light from outside of the focal plan. Essentially, the focal point of the light source and the focal point of the microscope's

B. Jeng (ed.), *Advances in Medical and Surgical Cornea: From Diagnosis to Procedure*, Essentials in Ophthalmology, DOI 10.1007/978-3-662-44888-5_4,

optical objective are aligned which allows very high resolution of cells.

Due to the pinhole, the field of view of such a design is very small and a full field of view must be built up by scanning, described by Petran et al. (1986). It can be by rotating a disk with thousands of optically conjugate source-detector pinholes in a spiral pattern, as in tandem scanning. The scanning mirror type of confocal microscope uses an optical slit, which scans the field by mechanically moving a slit beam via a mirror system (Koester 1991). Some of the confocal systems use a laser light source, while other confocal microscopes use a white-light source.

The images captured are oriented parallel to the surface of the tissue. The microscope has the ability to quickly adjust in the z-axis and scan through the tissue. Video and digital imaging capabilities are available on the microscope, which allows the examiner to scan through the full thickness cornea after acquisition. This technique also permits the 3-dimensional reconstruction of the cornea, as well as the study of the images in time (Cavanaugh et al. 1993; Petroll et al. 1993).

Limitations of the technique include the necessity to obtain multiple sections to evaluate larger areas of the cornea and the time of image acquisition and processing. Time to acquire a single image is typically less than 1/30 s, and the observation time in clinical settings is around 5 min.

4.2.2 Normal Anatomy

Sections obtained are oriented parallel to the surface of the tissue being imaged by confocal microscopy. Clinicians generally learn corneal anatomy in sections perpendicular to the surface (coronal sections). Thus, the examiner must learn normal corneal tissue appearance at different depths of the cornea, which are oriented parallel to the surface, in order to evaluate the specimen. All layers of the corneal tissue can be imaged, including the structures that run through the layers and between layers, such as nerves, blood vessels, and keratocytes. It is also important to understand that densities of cells and nerves can differ depending on the depth and central versus eccentric locations within the cornea.

The surface epithelium appears as a cellular mosaic with bright, hyper-reflective central nuclei. The cells of the basal epithelium are smaller and nuclei are not visible. Bowman's layer appears as an amorphous membrane and is best identified by the subbasal nerve plexus that lies beneath the Bowman's layer. This nerve plexus appears as a fine filamentous membrane. The stroma is composed of hyper-reflective, "bean-shaped" keratocyte nuclei, with density greatest just posterior to Bowman's layer and decreasing posteriorly (Prydal et al. 1998). The keratocyte cell bodies become visible when the keratocyte is activated. Nerves are seen running through the stroma and are larger compared to the more superficial nerves. Descemet's membrane is not visible on confocal microscopy unless significant fibrosis is present. The endothelium is composed of hexagonal cells with bright cells bodies with dark borders, similar to specular microscopy (Fig. 4.1) (Dhaliwal et al. 2007; Kitzmann et al. 2005; Cavanaugh et al. 1990).

The depth of each image within the cornea may also be recorded. This can help determine the depth of scars, foreign bodies, or location of infectious agents within the tissue.

Other uses of confocal microscopic imaging of the anterior segment has included imaging of the conjunctiva, lids, and corneoscleral limbus (Pichierri et al. 2008; Patel et al. 2006).

4.2.3 Clinical Uses

One of the major advantages of confocal microscopy is the ability to perform in vivo imaging without the need to mechanically section the cornea or use of stains or dyes (Lemp et al. 1985). The confocal microscopy examination can be performed comfortably on a cooperative patient in the clinical setting. The use of confocal microscopy has been described in many pathological conditions including infection, hereditary disorders (dystrophies), refractive, surgical, and other

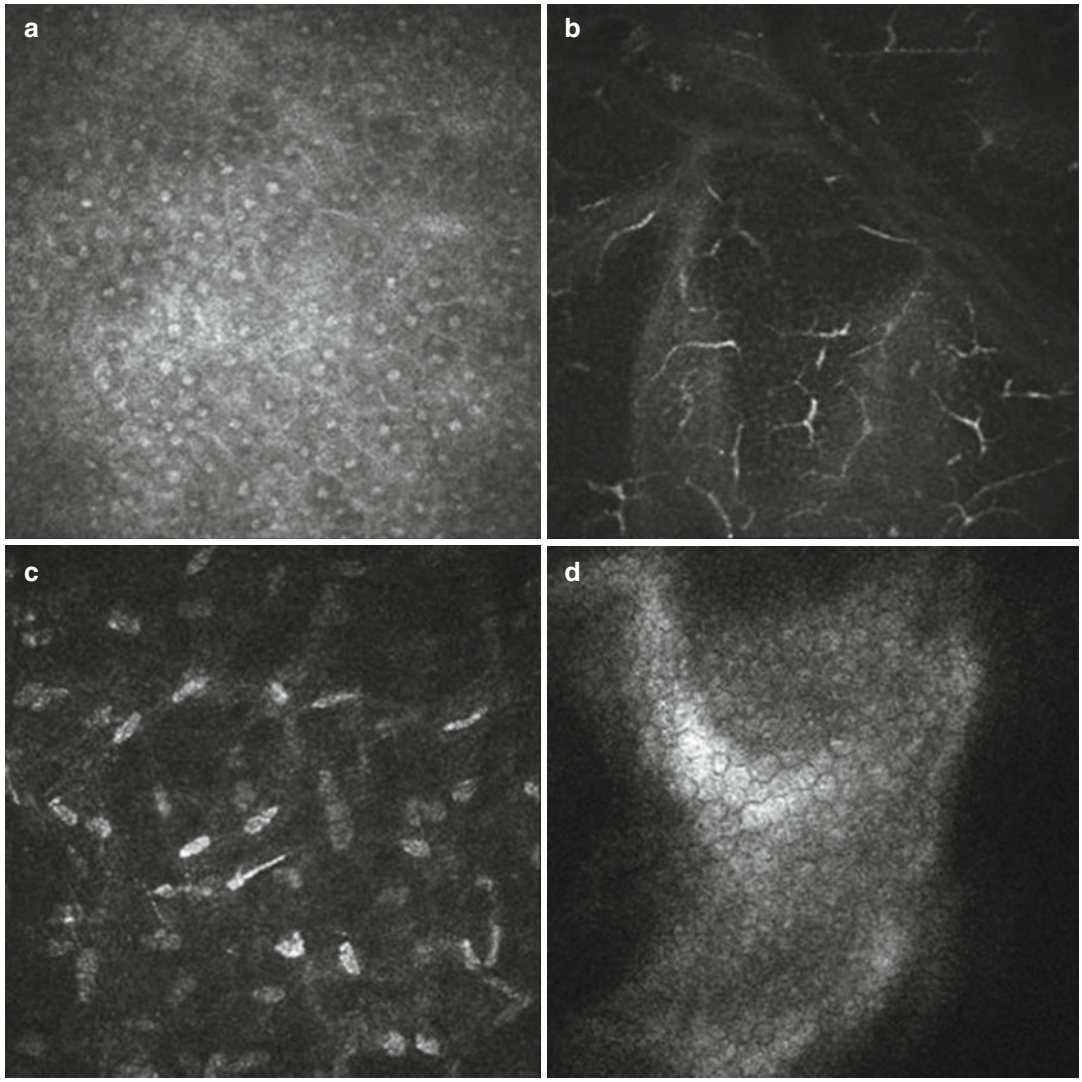

Fig. 4.1 Corneal layers as imaged with the confocal microscope. Corneal epithelium: seen with bright nuclei, (**a**); subbasal nerve plexus, (**b**); corneal stroma with keratocytes, (**c**); corneal endothelium with hexagonal cell borders, (**d**)

miscellaneous uses (Cavanagh et al. 1993). In clinical practice, confocal microscopy has been used to identify *Acanthamoeba* cysts and trophozoites, bacteria, fungi, and other pathogens within the cornea. In clinical research, it can be used for evaluation of responses and complications after refractive procedures, corneal wound healing processes, and a variety of corneal diseases.

Confocal microscopy has been shown to be useful in the diagnosis of *Acanthamoeba* keratitis (Mathers et al. 2000). The appearance of the cystic form of the organism is distinct using this imaging modality. The cyst is a double-walled hexagonal, hyper-reflective structure measuring approximately 10–30 μm in diameter. There may be a surrounding lucent area, representing a microcavitation of the stroma (Fig. 4.2). The trophozoite form can also be seen; however, it is more difficult to discern from surrounding normal keratocyte nuclei. Uniquely, the organism has been shown to be associated with corneal nerves, representing a radial keratoneuritis (Pfister et al. 1997). Confocal microscopy can also help guide

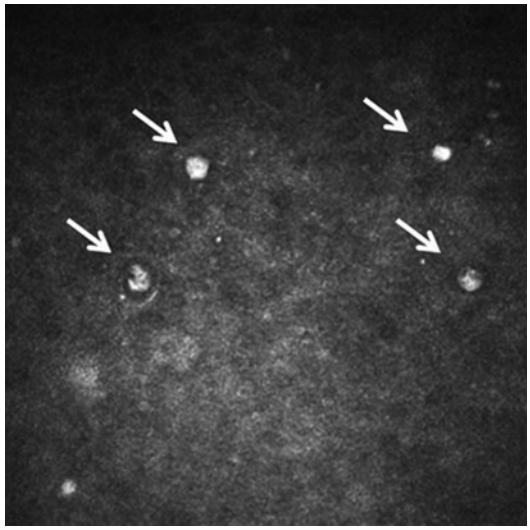

Fig. 4.2 Group of *Acanthamoeba* cysts in the epithelium (*arrows*). Note the hyper-reflective *Amoeba* with a lucent area and a surrounding bright halo

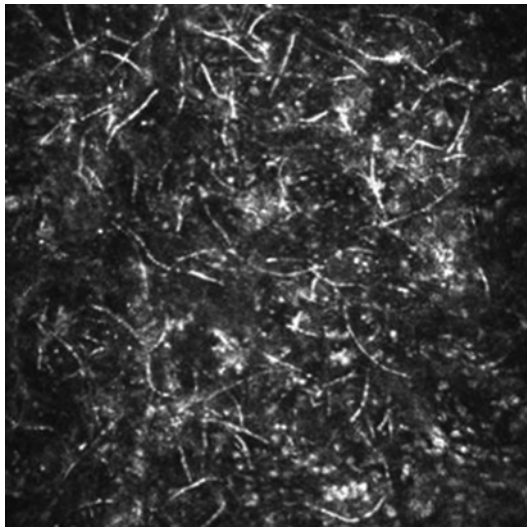

Fig. 4.3 Fungal filaments as imaged by confocal microscopy. Note the hyper-reflective filamentous elements. This fungus was identified as *Alternaria* species, by culture

the clinician in the treatment response in this notoriously difficult to treat condition.

Fungal keratitis has also been explored with the confocal microscope. The organisms are characterized by hyper-reflective filaments or budding forms (Fig. 4.3). The filaments appear to spread parallel to the surface of the cornea, possibly along the lamella of the cornea. There appears to be a role for confocal microscopy for diagnostic purposes (Winchester et al. 1997) especially in cases of deep infection, where a simple culture is not possible.

Due to the small size, most bacteria types cannot be distinguished by confocal microscopy. On exception is the filamentous bacteria, *Nocardia asteroids*, which appears as a hyper-reflective beaded, branching filaments. The branching typically occurs at right angles (Vaddavalli et al. 2006). Aggregates of bacteria have also been seen (Kaufman et al. 1996).

Although viruses cannot be visualized, the inflammatory patterns that accompany many such infections have been described. The subepithelial infiltrates seen after epidemic keratoconjunctivitis can be seen as hyper-reflective Langerhans cells in the basal epithelium and anterior stroma. Hyper-reflective fusiform cells (activated keratocytes) and round cells (inflammatory cells) have been reported in herpes simplex keratitis (Rosenberg et al. 2002).

Confocal microscopy has been used to evaluate postoperative complications in ophthalmic surgery. Examples include epithelial downgrowth after penetrating keratoplasty (Chen et al. 2013) and confirmation of retained Descemet's membrane following penetrating keratoplasty (McVeigh et al. 2013). In epithelial downgrowth, the observer would look for round hyper-reflective nuclei consistent with the epithelium at the level of the endothelium. After penetrating keratoplasty, a decrease in the density of cells at every level of the transplanted cornea has been reported (Niederer et al. 2007).

In the setting of refractive surgery, confocal microscopy has been used to study wound healing as well as surgical complications (Kaufman and Kaufman 2006). Corneal haze after phototherapeutic keratectomy (PRK) has been shown to be correlated with the presence of activated keratocytes (Moller-Pederson et al. 2000). Larger treatments with deeper ablations were noted to have increased numbers of activated keratocytes that remained activated longer. Corneal nerve density has been shown to significantly decrease after PRK but recovered by 24 months to presurgical levels (Erie 2003).

In laser-assisted in situ keratomileusis (LASIK), corneal nerve density has been shown to decrease significantly after 1, 2, and 3 years, not recovering to near preoperative densities until 5 years after surgery (Erie et al. 2005). This may be a significant cause of dry eye experienced after LASIK.

Various corneal dystrophies have been described. Epithelial basement dystrophy, lattice, Schnyder's crystalline, Thiel-Behnke, Reis-Bucklers, granular, and Fuchs' endothelial dystrophies are some of those characterized with confocal microscopy (Rosenberg et al. 2000; Kobayashi et al. 2003, 2009; Werner et al. 1999; Kaufman et al. 1993). The appearance of the Fuchs' endothelial dystrophy on confocal microscopy is similar to the appearance on specular microscopy with polymegathism and pleomorphism. However, one of the advantages of the confocal over specular microscopy in imaging Fuchs' is the ability to image through an edematous, hazy cornea, whereas with specular microscopy, the image cannot be obtained (Chiou et al. 1999a).

The confocal microscopy appearance of iridocorneal endothelial (ICE) syndrome demonstrates corneal endothelial cells consistent with the appearance of epithelial-like cells (Fig. 4.4) (Chiou et al. 1999b).

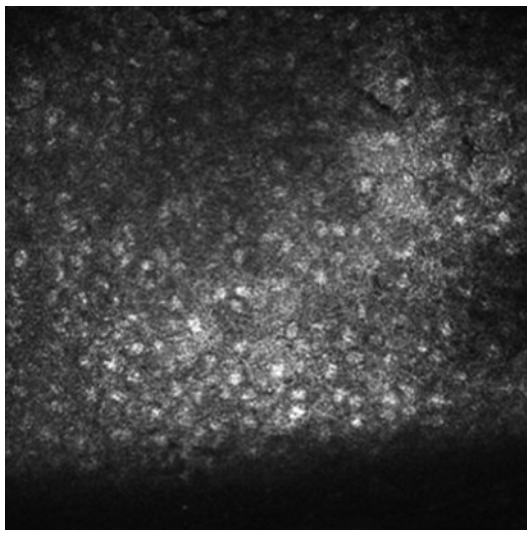

Fig. 4.4 Iridocorneal endothelial syndrome as imaged by confocal microscopy. Note epithelial-like cells with hyper-reflective nuclei at the level of the corneal endothelium

Confocal microscopy use in the cornea has also been described in systemic diseases such as diabetes in the evaluation and diagnosis of diabetic neuropathy (Chang et al. 2006) or in the evaluation of crystalline keratopathy in multiple myeloma (Mazzotta et al. 2014).

4.3 Specular Microscopy

In 1968, David Maurice developed specular microscopy, which then advanced to clinical use in 1975 with Bourne, Kaufman, and Laing (Maurice 1968; Bourne and Kaufman 1976). Specular microscopy is a technique that images tissue using light reflected from the optical interface of the corneal endothelium and the aqueous humor.

4.3.1 Normal Anatomy

Clinical specular microscopy provides quantitative assessment of endothelial cell density (ECD) and morphology as an indirect measure of function. Change in ECD is more important than an absolute value. Morphometric parameters provide information related to whether a cell population is under stress. The coefficient of variation (CV) measures a change in cell size (polymegathism), while % of hexagonal cells (% HEX) measures a change in cell shape (pleomorphism) (Fig. 4.5).

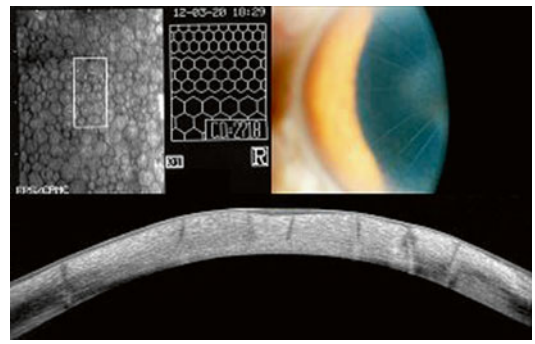

Fig. 4.5 Specular microscopy with anterior segment optical coherence tomography showing the endothelial mosaic after radial keratotomy surgery. Note with OCT the ability to identify the depth of each radial incision with epithelial remodeling

In most individuals, ECD decreases throughout life. Cell loss is most rapid from birth to the first few years of life. After the age of 60 years, ECD decreases significantly in most people, but there is a great degree of variability between individuals. On average, age-related cell loss is approximately 0.5 % per year (Sherrard et al. 1987). Though there is a large variation among age groups, most patients, even those greater than 70 years of age, should have an ECD of at least 2000 cells per mm^2, a coefficient of variation less than 0.40, and greater than 50 % hexagonal cells.

4.3.2 Clinical Uses

Specular microscopy is utilized in evaluating donor corneas, in identifying corneal dystrophies, and in providing valuable information for pre- and postsurgical management. Corneal edema is estimated to occur between 300 and 700 cells per mm^2 (Mishima 1982). Assuming cell loss in the range of 0–30 % for a given intraocular surgery, a patient should have at least 1,000–1,200 cells per mm^2 to safely undergo most anterior segment surgery without an increased risk of permanent postoperative corneal edema. When evaluating early postoperative corneas, imaging both centrally and in the midperiphery will identify regional disparities in ECD and morphology (Glasser et al. 1985). Reports of endothelial cell loss after cataract surgery using a variety of surgical approaches have demonstrated variable cell loss, but following uncomplicated phacoemulsification and posterior chamber intraocular lens implantation using viscoelastic and modern, small-incision techniques is low, ranging from no detectable cell loss to 20 % (Díaz-Valle et al. 1998).

Fuchs' endothelial corneal dystrophy (FECD) is a progressive, bilateral female predominant, endothelial disease that results in progressive corneal stromal edema and eventually epithelial edema and subepithelial fibrosis. The progressive morphologic changes of corneal guttae in FECD, with increased polymegathism and pleomorphism, initially start centrally (Laing et al. 1981). This has led many surgeons to utilize endothelial imaging to help predict postoperative outcomes.

The iridocorneal endothelial (ICE) syndrome, a unilateral female predominant, nonfamilial, progressive group of disorders, shows rounding of cell angles of the endothelium with a loss of cellular definition and a prevalence of pentagonal cells which are smaller than normal while also showing reversal of reflectivity (Sherrard et al. 1991). In contradistinction, posterior polymorphous corneal dystrophy (PPCD), a bilateral, nonprogressive, autosomal dominant disease, clinically appears similar to ICE syndrome, which complicates the diagnosis. However, using specular microscopy, the vesicles of PPCD have a thick dark border in a doughnut-like appearance with the lesion anterior to the endothelium and can be used to differentiate PPCD from ICE syndrome (Brooks et al. 1989).

Many investigators have studied photorefractive keratectomy (PRK) and laser-assisted in situ keratomileusis (LASIK) effects on the corneal endothelium. Most have shown that neither LASIK nor PRK results in a decreased endothelial density; however, ablation of the stroma within 200 μm of the corneal endothelium results in endothelial structural changes and the formation of the amorphous substance deposited onto Descemet's membrane (Edelhauser 2000).

In the Specular Microscopy Ancillary Study (SMAS) of the multicenter Cornea Donor Study (CDS) evaluating penetrating keratoplasty, endothelial cell loss from baseline to 5 years reached a staggering 70 % postoperatively. This does not directly correlate with functional status as in the SMAS; 14 % of the subjects with clear grafts had an ECD below 500 cells/mm^2. The study did note that cell loss continues throughout the life of the graft with highest correlation of long-term graft success using ECD at 6 months (Lass et al. 2010).

Endothelial keratoplasty (EK) has rapidly become the primary procedure for endothelial dysfunction since 2005 nearly surpassing penetrating keratoplasty in 2011 and increasing the gap in 2012. In 2013, the EBAA reported 24,987 cases of endothelial keratoplasty were performed. The procedure has been applied to all endothelial failure conditions, the cause for 40 % of all

corneal transplants in the United States (Eye Bank Association of America 2013). Most authors have reported significantly greater cell loss in the first 6 months after EK compared to PKP. Interestingly, although there is greater loss at 1 year when compared to PKP, the rate of cell loss begins to level off around 6 months, unlike PKP, as observed by several authors. After 1 year, there is minimal loss to the second and third years, 7 % between 6 months and 2 years, and 8 % between 6 months and 3 years, compared with 42 % in the eyes that underwent PKP in the Specular Microscopy Ancillary Study (SMAS) of the Cornea Donor Study (CDS) (Lass et al. 2010; Price and Price 2009).

In type I diabetes the cell density significantly decreases with age. Diabetic corneas also exhibit increased polymegathism and pleomorphism and a decreased percentage of hexagonality (Schultz et al. 1984).

4.4 Anterior Segment Optical Coherence Tomography

Anterior segment optical coherence tomography (OCT) is a high-resolution cross-sectional imaging modality, initially developed for retinal imaging at 830 nm (Huang et al. 1991). Applications for the anterior segment were first described in 1994 by Izatt et al. (1994). Due to limited penetrating through scattering tissue in the anterior segment, a longer wavelength was developed – 1,310 nm.

We have just begun to realize and appreciate the many applications of AS-OCT. Like high-resolution posterior segment OCT, clinicians are now recognizing the significance of AS-OCT for diagnosing, monitoring progression, and clinical decision-making.

4.4.1 Function

The anterior segment OCT is a light-based instrument, based on infrared light that segments ocular structures based on their reflectivity (indexes of refraction) – the ratio between light wave energy reflecting from the surface and light wave energy striking the same interface. Light at 1,310 is strongly absorbed by water. Less than 7 % of light on the cornea reaches the retina resulting in the ability of safely using a much higher power level (15 mW vs. 0.7 mW retina). Using 20× more power for anterior segment scanning equates to 20× faster scanning without sacrificing signal level. The longer wavelength also equals reduced scattering in opaque tissues such as the limbus, sclera, and iris. Also, the longer wavelength allows deeper penetration of the limbus for visualization of the scleral spur and angle recess (Huang et al. 1991).

Concentric or "arc" scanning produces uniformly strong reflections from the anterior and posterior corneal surfaces as well as the stromal collagen lamellae.

This scan maintains nearly perpendicular incidence angle as the OCT beam is scanned in the transverse dimension along collagen lamellae. The strong reflections from these normal structures reduce contrast for corneal scars and LASIK flap interface, making the visualization of these features difficult. Scan width is limited to a fraction of the diameter of the objective lens (Steinert and Huang 2008).

"Rectangular" or "telecentric" scanning produces the least image distortion and provides a range of useful contrast for corneal imaging. At the corneal vertex, the strong specular reflection offers a precise corneal landmark (Fig. 4.6). In the periphery, normal corneal surface and lamellar reflection fade but still remain visible (Steinert and Huang 2008).

Potential limitations include penetration through pigment and imaging the sulcus, zonules, and ciliary body. Image processing, compensation for corneal refraction, and patient fixation are potential causes of artifact. The unprocessed image is distorted by the indexes of refraction at the air-cornea and cornea-aqueous interfaces. Distortion is removed, "dewarping", by the computer software using Fermat's principle.

To achieve precision measurement of very fine anatomic structures, scans must be properly aligned and processed. Wavelength of 1,310 nm provides deeper penetration into tissues, approximately

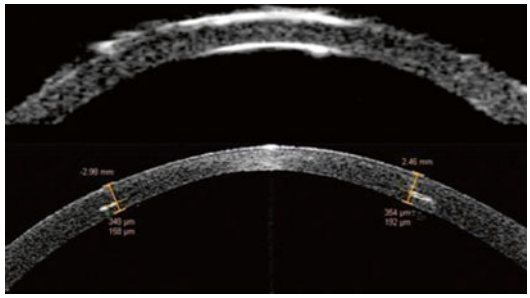

Fig. 4.6 Comparison of ultrasound biomicroscopy above with anterior segment OCT below. Note the resolution of the OCT allowing for identification of a corneal interface with scarring not visualized with ultrasound

18 μm axially. Because of the reduced scattering, AS-OCT can better penetrate turbid tissue of the sclera, angle, and iris. While wavelengths of 830 nm produce a greater axial resolution of approximately 3–5 μm, conversely, the shorter wavelength results in poorer penetration through opaque tissue and a shallow depth of view. Some examiners find the shallower 830 nm best suited for corneal examination (Radhakrishnan et al. 2001).

4.4.2 Clinical Uses

Applications for AS-OCT include corneal measurements, preoperative evaluation for implantation of intracorneal ring segments, angle closure assessment, and review of iris and crystalline lens position. AS-OCT is commonly used as a less invasive form of dynamic gonioscopy, post-iridotomy imaging, post-surgical management of trabeculectomy and/or shunt patency, as well as proving in-depth, high-resolution images of the cornea and anterior chamber. With proper examination and applied metric tools, one can grade the angle as well as the central anterior chamber depth. Most AS-OCT systems also provide pachymetry for central corneal thicknesses, as well (Asrani et al. 2008).

To fully realize the advantages of high-resolution imaging, the Fourier-domain OCT allows improved visualization of pathologic changes in the anterior segment such as corneal guttae, lattice lines, subepithelial changes, and irregular Bowman's layer (Wylegala et al. 2009).

Fig. 4.7 Anterior segment OCT in ICE syndrome showing angle closure and peripheral anterior synechiae with an associated slit lamp photo

4.4.3 AS-OCT Versus UBM

In general, due to its significant advantage of resolution (3–5 μm) versus that of UBM (100 μm), AS-OCT is the better choice for most anterior segment structures (Figs. 4.6 and 4.7).

Besides AS-OCT, ultrasound biomicroscopy (UBM) may also be used for cross-sectional imaging of the anterior segment and the AC angle. When compared to AS-OCT, UBM has the unique advantage of enabling visualization of structures posterior to the iris such as the ciliary body, zonules, and the peripheral lens. However, UBM is relatively more uncomfortable, requires a highly skilled operator in order to obtain good quality images, and has a limited scan width (5 × 5 mm) with the traditional UBM devices. This rarely provides significant advantages except in cases of severe corneal opacification where these other imaging modalities do not penetrate.

Conclusions

No one imaging technique can provide all the information to completely evaluate the cornea. While we strive for imaging that provides anatomical evaluation, we look forward to imaging systems that may also provide the opportunity to evaluate functional status of the cornea as well. Each imaging modality works together with the others to encompass the near complete story of the cornea. AS-OCT imaging provides

the clinician with tools for rapid in vivo cross-sectional imaging of the cornea and anterior segment. In addition to established uses for various corneal and iris diseases and disorders, promising work is being done with iris volume and anterior chamber volume studies. Recently there has been increasing interest in assessing dynamic factors such as iris volume that may identify eyes that are a risk of acute primary angle closure.

AS-OCT imaging provides the clinician in vivo cross-sectional imaging of the cornea and anterior segment. The uses are numerous. Further studies will continue to add to the diagnostic utility of this instrument in the clinic.

Confocal microscopy offers the clinician and researcher in vivo imaging of the cornea at cellular-level resolution. The uses are numerous. Further studies will continue to add to the diagnostic utility of this instrument in the clinic.

Compliance with Ethical Requirements

Conflict of Interest

Alla Kelly, MD; Stephen C. Kaufman, MD, PhD; Jonathan Lass MD; Denice Barsness, CRA, COMT, ROUB, CDOS, FOPS; Beth Ann Benetz, CRA, FOPS; and Pankaj Gupta, MD, MS declare that they have no conflict of interest related to the subject matter in the chapter.

Informed Consent

(2) No human studies were carried out by the authors for this article.

Animal Studies

(2) No animal studies were carried out by the authors for this article.

References

Asrani S, Sarunic M, Santiago C, Izatt J. Detailed visualization of the anterior segment using fourier-domain optical coherence tomography. Arch Ophthalmol. 2008;126(6):765–71.

Bourne WM, Kaufman HE. Specular microscopy of human corneal endothelium in vivo. Am J Ophthalmol. 1976;81(3):319–23.

Brooks AM, Grant G, Gillies WE. Differentiation of posterior polymorphous dystrophy from other posterior corneal opacities by specular microscopy. Ophthalmology. 1989;96(11):1639–45.

Cavanagh HD, Petroll WM, Alizadeh H, He YG, McCulley JP, Jester JV. Clinical and diagnostic use of in vivo confocal microscopy in patients with corneal disease. Ophthalmology. 1993;100(10):1444–54.

Cavanaugh HD, Jester JV, Essepian J, Shields W, Lemp MA. Confocal microscopy of the living eye. CLAO J. 1990;16(1):65–73.

Cavanaugh HD, Petroll WM, Jester JV. The application of confocal microscopy to the study of living systems. Neurosci Biobehav Rev. 1993;17(4):483–98.

Chang PY, Carrel H, Huang JS, Wang IJ, Chen WL, Wang JY, Hu FR. Decreased density of corneal basal epithelium and subbasal corneal nerve bundle changes in patients with diabetic retinopathy. Am J Ophthalmol. 2006;142(3):488–90.

Chen MC, Cortes DE, Harocopos G, Mannis MJ. Epithelial downgrowth after penetrating keratoplasty: imaging by high-resolution optical coherence tomography and in vivo confocal microscopy. Cornea. 2013;32(11):1505–8.

Chiou AG, Kaufman SC, Beuerman RW, Ohta T, Soliman H, Kaufman HE. Confocal microscopy in corneal guttata and Fuchs' endothelial dystrophy. Br J Ophthalmol. 1999a;83(2):185–9.

Chiou AG, Kaufman SC, Beuerman RW, Ohta T, Yaylali V, Kaufman HE. Confocal microscopy in the iridocorneal endothelial syndrome. Br J Ophthalmol. 1999b;83(6):697–702.

Dhaliwal JS, Kaufman SC, Chiou AGY. Current applications of clinical confocal microscopy. Curr Opin Ophthalmol. 2007;18(4):300–7.

Díaz-Valle D, Benítez del Castillo Sánchez JM, Castillo A, Sayagués O, Moriche M. Endothelial damage with cataract surgery techniques. J Cataract Refract Surg. 1998;24(7):951–5.

Edelhauser HF. The resiliency of the corneal endothelium to refractive and intraocular surgery. Cornea. 2000;19(3):263–73.

Erie JC. Corneal wound healing after photorefractive keratectomy: a 3-year confocal microscopy study. Trans Am Ophthalmol Soc. 2003;101:293–333.

Erie JC, McLaren JW, Hodge DO, Bourne WM. Recovery of corneal subbasal nerve density after PRK and LASIK. Am J Ophthalmol. 2005;140(6):1059–64.

Eye Bank Association of America. 2013 Eye Banking Statistical Report. 2008. http://www.restoresight.org/wp-content/uploads/2013/04/2012_Statistical_Report_FINAL-reduced-size-4-10.pdf

Glasser DB, Matsuda M, Gager WE, Edelhauser HF. Corneal endothelial morphology after anterior chamber lens implantation. Arch Ophthalmol. 1985;103(9):1347–9.

Huang D, Swanson EA, Lin CP, et al. Optical coherence tomography. Science. 1991;254:1178–81.

Izatt JA, Hee MR, Swanson EA, et al. Micrometer-scale resolution imaging of the anterior eye in vivo with

optical coherence tomography. Arch Ophthalmol. 1994;112:1584–9.
Kaufman SC, Kaufman HE. How has confocal microscopy helped us in refractive surgery? Curr Opin Ophthalmol. 2006;17:380–8.
Kaufman SC, Beuerman RW, Kaufman HE. Diagnosis of advanced Fuchs' endothelial dystrophy with the confocal microscope. Am J Ophthalmol. 1993;116(5):652–3.
Kaufman SC, Laird JA, Cooper R, Beuerman RW. Diagnosis of bacterial contact lens related keratitis with the white-light confocal microscope. CLAO J. 1996;22(4):274–7.
Kitzmann AS, Winter EJ, Nau CB, McLaren JW, Hodge DO, Bourne WM. Comparison of corneal endothelial cell images from a noncontact specular microscope and a scanning confocal microscope. Cornea. 2005;24(8):980–4.
Kobayashi A, Sakurai M, Shirao Y, Sugiyama K, Ohta T, Amaya-Ohkura Y. In vivo confocal microscopy and genotyping of a family with Thiel-Behnke (honeycomb) corneal dystrophy. Arch Ophthalmol. 2003;121(10):1498–9.
Kobayashi A, Fujiki K, Murakami A, Sugiyama K. In vivo laser confocal microscopy findings and mutational analysis for Schnyder's crystalline corneal dystrophy. Ophthalmology. 2009;116(6):1029–37.
Koester C. Scanning mirror microscope with optical sectioning characteristics: applications in ophthalmology. Appl Opt. 1980;19:1749–57.
Laing RA, Leibowitz HM, Oak SS, Chang R, Berrospi AR, Theodore J. Endothelial mosaic in Fuchs' dystrophy. A qualitative evaluation with the specular microscope. Arch Ophthalmol. 1981;99(1):80–3.
Lass JH, Sugar A, Benetz BA, et al. Endothelial cell density to predict endothelial graft failure after penetrating keratoplasty. Arch Ophthalmol. 2010;128(1):63–9.
Lemp MA, Dilly PN, Boyde A. Tandem-scanning (confocal) microscopy of the full thickness cornea. Cornea. 1985–1986;4(4):205–9.
Mathers WD, Sutphin JE, Folberg R, et al. Confirmation of confocal microscopy diagnosis of Acanthamoeba keratitis using polymerase chain reaction analysis. Arch Ophthalmol. 2000;118:178–83.
Maurice DM. Cellular membrane activity in the corneal endothelium of the intact eye. Experientia. 1968;24(11):1094–5.
Mazzotta C, Caragiuli S, Caporossi A. Confocal microscopy in a case of crystalline keratopathy in a patient with smouldering multiple myeloma. Int Ophthalmol. 2014;34(3):651–4.
McVeigh K, Cornish KS, Reddy AR, Vakros G. Retained Descemet's membrane following penetrating keratoplasty for Fuchs' endothelial dystrophy: a case report of a post-operative complication. Clin Ophthalmol. 2013;7:1511–4.
Minsky M. Memoir on inventing the confocal microscope. Scanning. 1988;10:128–38.
Mishima S. Clinical investigations on the corneal endothelium. Ophthalmology. 1982;89(6):525–30.
Moller-Pederson T, Cavanaugh HD, Petroll WM, Jester JV. Stromal wound healing explains refractive instability and haze development after photorefractive keratectomy: a 1-year confocal microscopic study. Ophthalmology. 2000;107(7):1235–45.
Naroo SA, Cervino A. Corneal topography and its role in refractive surgery. In: Narco SA, Butterworth H, editors. Refractive surgery: a guide to assessment and management. London: Elsevier; 2004. p. 9–16.
Niederer R, Perumal D, Sherwin T, et al. Corneal innervation and cellular changes after corneal transplantation: an in vivo confocal microscopy study. Invest Ophthalmol Vis Sci. 2007;48:621–6.
Patel DV, Sherwin T, McGhee CNJ. Laser scanning in vivo confocal microscopy of the normal human corneoscleral limbus. Invest Ophthalmol Vis Sci. 2006;47(7):2823–7.
Petran M, Hadravsky M, Egger MD, Galambos R. Tandem-scanning reflected-light microscope. J Opt Soc Am. 1968;58:661–4.
Petran M, Hadravsky M, Benes J, Boyde A. In vivo microscopy using the tandem scanning microscope. Ann N Y Acad Sci. 1986;483:440–7.
Petroll WM, Cavanaugh HD, Jester JV. Three-dimensional imaging of corneal cells using in vivo confocal microscopy. J Microsc. 1993;170(Pt 3):213–9.
Pfister DR, Cameron JD, Krachmer JH, Holland EJ. Confocal microscopy findings of Acanthamoeba keratitis. Am J Ophthalmol. 1997;115:714–8.
Pichierri P, Martone G, Loffredo A, Traversi C, Polito E. In vivo confocal microscopy in a patient with conjunctival lymphoma. Clin Experiment Ophthalmol. 2008;36(1):67–9.
Price Jr FW, Price MO. Does endothelial cell survival differ between DSEK and standard PK? Ophthalmology. 2009;116(3):367–8.
Prydal JI, Franc F, Dilly PN, Kerr Muir MG, Corbett MC, Marshall J. Keratocyte density and size in conscious humans by digital image analysis of confocal images. Eye (Lond). 1998;12(pt 3a):337–42.
Radhakrishnan S, Rollins AM, Roth JE, et al. Real-time optical coherence tomography of the anterior segment at 1310 nm. Arch Ophthalmol. 2001;119:1179–85.
Rosenberg ME, Tervo TM, Petroll WM, Vesaluoma MH. In vivo confocal microscopy of patients with corneal recurrent erosion syndrome or epithelial basement membrane dystrophy. Ophthalmology. 2000;107(3):565–73.
Rosenberg ME, Terno TM, Muller LJ, Moilanen JA, Vesaluoma MH. In vivo confocal microscopy after herpes keratitis. Cornea. 2002;21(3):265–9.
Schultz RO, Matsuda M, Yee RW, Edelhauser HF, Schultz KJ. Corneal endothelial changes in type I and type II diabetes mellitus. Am J Ophthalmol. 1984;98(4):401–10.
Sherrard ES, Novakovic P, Speedwell L. Age-related changes of the corneal endothelium and stroma as seen in vivo by specular microscopy. Eye (Lond). 1987;1(Pt 2):197–203.

Sherrard ES, Frangoulis MA, Muir MG. On the morphology of cells of posterior cornea in the iridocorneal endothelial syndrome. Cornea. 1991;10(3):233–43.

Steinert R, Huang D. Anterior segment optical coherence tomography. 1st ed. Thorofare: Slack Inc.; 2008.

Vaddavalli PK, Garg P, Sharma S, Thomas R, Rao GN. Confocal microscopy for Nocardia keratitis. Ophthalmology. 2006;113(9):1645–50.

Werner LP, Werner L, Dighiero P, Legeais JM, Renard G. Confocal microscopy in Bowman and stromal corneal dystrophies. Ophthalmology. 1999;106(9):1697–704.

Winchester K, Mathers WD, Sutphin JE. Diagnosis of Aspergillus keratitis in vivo with confocal microscopy. Cornea. 1997;16:27–31.

Wylegala E, Teper S, Nowinska AK, Milka M, Dobrowolski D. Anterior segment imaging: Fourier-domain optical coherence tomography versus time-domain optical coherence tomography. J Cataract Refract Surg. 2009;35(8):1410–4.